Hydrology and Earth System Sciences Discussions

Papers published in *Hydrology and Earth System Sciences Discussions* are under open-access review for the journal *Hydrology and Earth System Sciences*

Parameterization of the coupling CO_2 and H_2O gas exchange model at the leaf scale of *Populus euphratica* tree

G. Zhu[1,2], X. Li[1], Y. Su[1], and C. Huang[1]

[1]Cold and Arid Regions Environmental and Engineering Research Institute, Chinese Academy of Sciences, Lanzhou 730000, China
[2]The School of Mathematics, Physics & Software Engineering, Lanzhou Jiaotong University, Lanzhou, 730000, China

Correspondence to: G. Zhu (syh@lzb.ac.cn)

HESSD

6, 6503–6534, 2009

Parameterization of the coupling CO_2 and H_2O exchange model

G. Zhu et al.

Title Page

Abstract	Introduction
Conclusions	References
Tables	Figures

| I◄ | ►I |
| ◄ | ► |

| Back | Close |

Full Screen / Esc

Printer-friendly Version

Interactive Discussion

Abstract

The following two models were combined to predict simultaneously CO$_2$ and H$_2$O gas exchange at the leaf scale of *Populus euphratica*: a Farquhar et al. type biochemical sub-model of photosynthesis (Farquhar et al., 1980) and a Ball et al. type stomatal conductance sub-model (Ball et al., 1987). The photosynthesis parameters, $V_{c\,\mathrm{max}}$, J_{max}, TPU, and R_d (maximum carboxylation rate allowed by ribulose 1·5-bisphosphate carboxylase/oxygenase (Rubisco), rate of phosynthetic electron transport, triose phosphate use, and day respiration) at the measurement temperature were determined by using the genetic algorithm (GA) method based on A/C_i data sets. The stomatal conductance sub-model was calibrated independently. Prediction of net photosynthesis by the coupled model agreed well with the validation data, but the model tended to underestimate rates of transpiration. Overall, the combined model generally captured the diurnal patterns of CO$_2$ and H$_2$O exchange resulting from variation in temperature and irradiation.

1 Introduction

Recently, simultaneous estimations of CO$_2$ and H$_2$O gas exchange coupling the Farquhar et al. (1980) type biochemical model of photosynthesis and the Ball et al. (1987) type stomatal conductance model have been reported in many articles (e.g. Tenhunen et al., 1990; Collatz et al., 1991; Harley et al., 1992; Leuning, 1995; Sellers et al., 1996; De Pury and Farquhar, 1997; Baldocchi and Meyers, 1998; Wilson et al., 2001; Kosugi et al., 2003; Kim and Lieth, 2003). A major advantage of using the combined models with this framework is that it is mechanistic and, therefore, capable of describing the CO$_2$ and H$_2$O gas exchange processes that might not be well described by simple empirical approaches. The disadvantage is that it requires extensive calibration of a number of parameters (Cannell and Thornley, 1998). As for data, they are still insufficient and further studies of the variations in the parameters of both the photo-

synthesis and stomatal conductance models for various materials and environmental conditions are still needed, especially for the forest tree species in spite of their significance for gas exchange estimation at the land surface (Kosugi et al., 2003). There are only a few lists of these parameters for SiB2 (Sellers et al., 1996), one of the famous

5   global scale land surface models, which uses a Farquhar et al. (1980) type net assimilation model and a Ball et al. (1987) type stomatal conductance model, and more precise information on the gas exchange parameters are needed to evaluate the fluxes over the vegetations on ecologically relevant time scales. Moreover, the methods used in estimating the parameters of interest have not received much attention and need

10 further studies (Dubois et al., 2007).

Over the past two decades, the responses of net photosynthesis (A) to the leaf intercellular concentration (C_i), i.e. the A/C_i curve fitting analyses, have been widely used to parameterize leaf photosynthesis. These analyses have been invaluable for elucidating and quantifying in vivo the fundamental biochemical processes underlying the

15 photosynthetic responses of plants to various environmental conditions (von Caemmerer, 2000). However, this procedure of parametrization requires that each A/C_i set be first divided into several subsets and the parameters of the model are customarily estimated through separate fitting of the component functions corresponding to the three segments, rather than fitting all parameters simultaneously based on the entire

20 data set (Kim and Lieth, 2003). It should be noted that the identification of the cut-off point between different subsets is usually arbitrary, in the sense of the discretion of the investigator. The consequence of arbitrary subsetting of the data is that it creates an entry for systematic deviation from the true parameter values (Dubois et al., 2007). Moreover, measurement noise is inevitable in realistic testing conditions. However, the

25 A/C_i curve fitting method is sensitive to noisy data, and small or noise date sets will be subject to significant estimation problems (Sharkey et al., 2007). All these promote us to find an innovative method to parameterize the FvCB model, which can perfectly overcome the flaws of the A/C_i curve fitting method.

In general, parameter estimate can be viewed as an optimization problem. The

goal is the determination of a set of parameters which, substituted into a mathematical model, generate results consistent with measured experimental data. During the last three decades, there has been a growing interest in solving optimization problems by mimicking natural processes, such as biological evolution and metal annealing (Ooka and Komamura, 2009). Among them, the Genetic Algorithms (GA) pioneered by Holland (1975) is such a technique that has received considerable attention (Lee et al., 2006). Compared with traditional optimization methods (e.g. ordinary least squares, weighted and generalized least squares, Bayesian, and maximum likelihood method) relating to the parameter estimation, the GA is more appropriate when the function includes some complexities and/or discontinuities (Barth, 1992). Major advantages of the GA include that: (1) it has very good characteristics of robustness and global convergence; (2) it can process a large number of variables at the same time; (3) it can handle the nonlinearity between the model and its parameters; (4) it can be computed simply but does not need a sensitivity analysis and has a high implicit parallelism (Holland, 1975; Hu et al., 2007).

Populus euphratica, one of the oldest species of *Populus* in *Salicaceae*, is the sole species of the genus naturally growing at the edge of barren deserts or semi-barren deserts (Gu et al., 2004). Its high survival and biomass production in the arid areas of Mongolia, China, Pakistan, Iraq, and Iran is acclaimed (Sharma et al., 1999). *P. euphratica* is characterized by a great resistance to drought, high irradiance and temperature, wind, and salinity in the soils, and is very important in maintaining ecosystem function in arid and semi-arid regions (Chen et al., 2004). Comparative studies have been carried out to determine the responses of *P. euphratica* to salt and drought stress (Ma et al., 2002; Chen et al., 2004, 2006). However, efforts to use the gas-exchange data of *P. euphratica* leaves to determine the biochemical model parameters and their temperature dependences are missing or even non-existent. Furthermore, coupled gas exchange models have rarely been developed for *P. euphratica*.

In this study, the well-know combined model that simulates both CO_2 and H_2O gas exchange on a leaf scale was applied to several data sets obtained from in suit leaf-

scale observations of CO_2 and H_2O gas exchange of *P. euphratica* leaves, to parameterize the leaf characteristics related to the gas exchange using the GA method. Also, some details of implementation were provided. This information should be of interest to physiologists who seek to understand the enzymatic and photochemical events regulating CO_2 assimilation of the specific species, and modelers searching for species-specific estimates of photosynthesis parameters for use in describing large scales CO_2 and H_2O exchange.

2 Methods and materials

2.1 Model description

2.1.1 Photosynthesis, stomatal conductance and transpiration sub-models

The combined model used for the estimation consists of a Ball et al. (1987) type stomatal conductance sub-model (BWB model), a Farquhar et al. (1980) type biochemical sub-model of photosynthesis for C_3 plants (FvCB model) and the integrated sub-model of transpiration.

In FvCB model, the net CO_2 assimilation rate A could be modeled as the minimum of three limiting rates:

$$A = \min\{A_c, A_j, A_p\} - R_d \, , \tag{1}$$

A_c is the rate of photosynthesis when Rubisco activity is limiting, A_j is the rate when ribulose-1,5-bisphosphate (RuBP)-regeneration is limiting by electron transport, and A_p is the rate when triose phosphate utilization (TPU) is limiting. R_d is the rate of mitochondrial respiration. Rubisco-limited photosynthesis is given by:

$$A_c = V_{c\max} \left[\frac{C_i - \Gamma^*}{C_i + K_c(1 + O/K_o)} \right] \, , \tag{2}$$

HESSD

6, 6503–6534, 2009

Parameterization of the coupling CO$_2$ and H$_2$O exchange model

G. Zhu et al.

Title Page

Abstract	Introduction
Conclusions	References
Tables	Figures

|◄ | ►|

◄ | ►

| Back | Close |

Full Screen / Esc

Printer-friendly Version

Interactive Discussion

where $V_{c\,max}$ is the maximum rate of Rubisco activity, C_i and O are the intercellular concentrations of CO_2 and O_2 (21 kPa), respectively, K_c and K_o are the Michaelis-Menten coefficient of Rubisco activity for CO_2 and O_2, respectively, and Γ^* is the CO_2 compensation point in the absence of mitochondrial respiration. This formulation of the model assumes that the cell-wall conductance, the conductance between the intercellular space and the site of carboxylation, is negligible. Some authors have argued that this conductance is significant and may vary with leaf temperatures (e.g. Makino et al., 1994). For the species considered here, we did not have access to appropriate data to evaluate the cell-wall conductance and hence were obliged to use the form of the model given above.

The rate of photosynthesis when RuBP regeneration is limiting is given by:

$$A_j = J \frac{C_i - \Gamma^*}{4C_i + 8\Gamma^*} \,, \tag{3}$$

where J is the rate of electron transport. J is related to incident photosynthetically active photo flux density, Q, by:

$$\theta J^2 - (\alpha Q + J_{max})J + \alpha Q J_{max} = 0 \,, \tag{4}$$

where J_{max} is the potential rate of electron transport, θ is the curvature of the light response curve and α is the quantum yield of electron transport. The value of α was fixed at $0.3\,\mathrm{mol\,electrons\,mol^{-1}}$ photon, based on an average C_3 photosynthetic quantum yield of 0.093 and a leaf absorptance of 0.8 (Long et al., 1993). The value of θ was taken to be 0.90. These parameter values have only a slight effect on the estimated value of J_{max} (Medlyn et al., 2002).

When the rate of photosynthesis is limited by TPU, it is simply:

$$A_p = 3\,\mathrm{TPU} \,. \tag{5}$$

Where TPU is the rate of use of triose phosphates but can also be any export of carbon from the Calvin cycle, including direct use of photorespiratory glycine or serine.

The accuracy of the photosynthesis model depends on proper representation of the kinetic properties of Rubisco. Fortunately, the kinetic properties of Rubisco among C_3 plants have been shown to be relatively conserved and thus we use a general set of kinetic parameters (Table 1; see also von Caemmerer, 2000; Sharkey et al., 2007) but with caution (Tcherkez et al., 2006). There are four parameters that need to be estimated. These are $V_{c\,max}$, J_{max}, A_p and R_d corresponding to measurement temperatures, thus comparisons between two treatments are often made at a single temperature. Representative temperature responses of the fitted parameters are used to adjust these values to a single temperature in this case 25°C. The dependence of reaction rates on the temperature is exponential:

$$\text{Parameter} = e^{\left(c - \frac{\Delta Ha}{R \cdot T_k}\right)} \tag{6}$$

or

$$\text{Parameter} = \frac{e^{\left(c - \frac{\Delta Ha}{R \cdot T_k}\right)}}{1 + e^{\left(\frac{\Delta S \cdot T_k - \Delta H_d}{R \cdot T_k}\right)}} \ , \tag{7}$$

where c is a scaling constant, ΔH_a is an enthalpy of activation, ΔH_d is enthalpy of deactivation, ΔS is the entropy, T_k denotes leaf temperature in K and R is the universal gas constant (8.314 J mol^{-1} K^{-1}). The scaling constant for the equations used to adjust the parameters is chosen to cause the results to be 1 at 25°C and the calculated value at other temperature can be used to scale the parameter to 25°C. The values used in this paper are presented in Table 1.

In sub-model BWB, the stomatal conductance is estimated from the net assimilation rate (A), relative humidity (h), and CO_2 concentration at the leaf surface (C_s) using,

$$g_{sw} = m\frac{h}{C_s}A + g_{sw\,min} \tag{8}$$

where g_{sw} is the stomatal conductance of H_2O, m is the slope of the relationship between the stomatal index (Ah/C_s) and the stomatal conductance and $g_{sc\,min}$ is the

6509

minimum stomatal conductance. The CO_2 concentration at the leaf surface C_s is calculated using the CO_2 concentration of the air in the chamber.

Under steady-state conditions, C_i can be estimated using the stomatal conductance of CO_2 (g_{sc}):

$$C_i = C_s - \frac{A}{g_{sc}} \tag{9}$$

where, g_{sc} is the stomatal conductance to CO_2 such that $g_{sc} = \frac{g_{sw}}{1.6}$. The transpiration rate, E, can be calculated as,

$$E = g_{sw} \text{VPD}_s \tag{10}$$

where, VPD_s is the water vapor pressure deficit between intercellular space and the air layer just above the leaf surface.

2.1.2 Coupling the models

The FvCB model uses C_i, among others (T_k and Q), as driving variables. The BWB model requires the net photosynthesis A as an input, while C_i results from the interaction of A and g_{sw}. Therefore, the two sub-models are interdependent. A nested iterative procedure was used to solve this relation numerically (Fig. 1). In finding the solution, the value of C_i was assumed to be equal to $0.7C_a$, and substituted into the biochemical photosynthesis model (Eq. 1) and to obtain an estimate of A. Then stomatal conductance (g_{sc}) was calculated from the stomatal model (Eq. 11), and a new C_i was estimated using the resulting A and g_{sc} (Eq. 10). This process was solved iteratively using the Newton-Raphson method until the change in C_i was less than a certain small value of allowance. It should be noticed that the parameters of the FvCB sub-model must be calibrated firstly (discuss below).

2.2 Plant materials

The experiment was conducted at Qidaoqiao in Ejina, Inner Mogolia, China. The experiment site is located at 42°21′ N and 101°15′ E, with an altitude of 920.5 m a.s.l. This is one of the most arid regions in China, with evaporation exceeding 3500 mm year^{-1} and mean annual rainfall, 84% of which occurs during the growing season, is less than 50 mm year^{-1}. The annual mean air temperature is about 8.1°C. A winter minimum temperature of −38.5°C (17 January 1996) and a summer maximum of 43.1°C (21 July 1980) have been recorded, and an average diurnal temperature range is 28–30°C (Su et al., 2007). Prevailing winds are northwesterly in winter and spring, and southwesterly to southerly in summer and fall. Annual mean wind velocity ranges from 3.4 to 4.0 m s^{-1}. Total annual sunshine time is from 3170 to 3444 h, the accumulated temperature (≥10°C) is from 3549 to 3695°C.

Materials used in the experiment were 25-year-old, healthy and free of diseases and pest damages *P. euphratica* trees with a height of 8–10 m. The trees were accessed via a canopy access tower. Three to four intact dentate broad-ovate leaves on the sunny exposing side were selected for measurements. The measurements were conducted on 8, 10, 17 July 2006 which were all clear days.

2.3 Gas exchange measurement

A photosynthesis system (LI-6400; LI-COR, Lincoln, NE, USA) with a red/blue light source (LI6400-02B) mounted onto a 6 cm^2 clampe-on leaf chamber was used to determine light and A/C_i responses under various environment conditions. For the generation of A/C_i response curves, three leaf replicas were used. Prior to the measurement the leaf was acclimated to saturating irradiance (1500 μmol m^{-2} s^{-1}) and measurement temperature for half an hour. The CO_2 concentration in the cuvette was gradually decreased from 360 μmol mol^{-1} to about 20 μmol mol^{-1} through five steps, increased back to 360 μmol mol^{-1} and then the leaf was allowed to acclimate for at least five minutes. Upon completion of this sequence, the CO_2 concentration was increased to

about 1200 μmol mol^{-1} through six steps. The light response of leaves was determined at several irradiance levels between 0 and 1800 μmol m^{-2} s^{-1} at 25°C leaf temperature and 360 μmol mol^{-1} CO$_2$ inside the leaf chamber. For light response curves, measurements started with a leaf equilibrated to high light and the light level was then gradually decreased.

The A/C_i response of leaves was investigated at various leaf temperatures (10, 15, 20, 25, 30, 35 and 40°C) to determine the temperature dependence of the photosynthetic parameters. The leaf chamber was modified by replacing the peltier external heat sink with a metal block containing water channels, which in turn were connected to a heating/cooling circulating water bath (Endocal RTE-100, Neslab Instruments, Newington, USA). The modified heating/cooling blocks, used in conjunction with the peltier temperature controls, provided leaf temperature control at any preset value between 10–45°C. Leaf temperatures were measured using a chromal-constantin thermocouple pressed to the lower leaf surface. The temperatures reported by this particular thermocouple were cross-checked against standard mercury-in-glass thermometers in a controlled temperature chamber and found to be within ±0.4°C (Bernacchi et al., 2003).

Using 99 leaves, the response of g_{sc} to relative humidity (0.05–0.90), irradiance (>100 μmol m^{-2} s^{-1}), leaf temperature (10–40°C) and a range of CO$_2$ levels (>50 μmol mol^{-1}) was determined to calibrate the stomatal conductance model. Relative humidity was controlled by adjusting the flow rate of air through the leaf chamber. Measurements used to calibrate the stomatal conductance model were collected by waiting until the rate of C_i, transpiration and CO$_2$ assimilation had stabilized before taking reading; this wait-time ranged from 5 to 30 min depending on the leaves and the environmental conditions of the camber.

2.4 Parameter estimation

The objective of parameter calibration is to determine the parameters $\theta=[\theta_1, \theta_2, \cdots, \theta_h]'$ so that the values of the dependent variable calculated from the model $\eta=f(\theta, X)=[f_1(\theta, X), f_2(\theta, X), \cdots, f_l(\theta, X)]'$ best agree with those observed from experimentation $Y=[y_1, y_2, \cdots, y_l]'$. We define our objective function that derives the optimization procedure as,

$$\min S(\theta) = \sum_{j=1}^{l} \sum_{i=1}^{N_o} \left\{ w_j [y_j(i) - \eta_j(i)]^2 \right\} = \sum_{j=1}^{l} \sum_{i=1}^{N_o} \left\{ w_j [y_j(i) - f_j(\theta, X(i))]^2 \right\} , \qquad (11)$$

where l is the estimated outputs, $X=[x_1(i), x_2(i), \cdots, x_n(i)]'$ is the input variables, and N_0 is the number of data sets. In the present work we used the GA to find a vector θ in the given search space, which is defined by providing the lower and upper bounds for each of the $h \times 1$ dimensions of θ, i.e., $\theta^{min} \leq \theta \leq \theta^{max}$ (discussed below).

The GA is effective stochastic global that mimic biological evolution. As it is robust, i.e., it uses only objective function information and not other auxiliary information, it has been successfully applied to various problems, such as function optimization and combinatorial optimization, especially when a rigorous mathematical model is too complicated to be practically implemented (Goldberg, 1989). The basic operations involved in a GA include three basic operators: selection, crossover, and mutation. The linkage between the coupling model and the GA is shown in Fig. 2. The procedure is summarized as follows: first, an initial set (called a "population") of vectors (called "individuals") whose elements (called "genomes") are the values of the parameters is generated. This population is a representative set of solutions to the problem under investigation. Each individual is evaluated on its performance with respect to the fitness function. For parameter estimation problems, the fitness of a particular individual is roughly proportional to the inverse of the errors between experimental and predicted values ($S(\theta)$). Using this measure, the individual competes in a selection process where the fittest survives and is selected to enter the mating pool; the lesser-fit indi-

vidual dies. The selected individuals (parents) are assigned a mate randomly. Genetic information is exchanged between the two parents by crossover to form offspring. The parents are then killed and replaced in the population by the offspring to keep the population size stable. Reproduction between the individuals takes place with a probability of crossover. If a random number generated is less than the probability of crossover, crossover happens, otherwise not, and the parents enter into the new population. GA is very aggressive search techniques; they tend to converge quickly to a local optimum if the only genetic operators used are selection and crossover. The reason is that GA eliminates rapidly those individuals with poor measures until all the individuals in the population are identical. Without a fresh influx of new genetic materials, the solution stops there. To maintain diversity, some of the genes are subjected to mutation to keep the population from premature convergence (Goldberg, 1989; Cieniawski et al., 1995). Selection, crossover and mutation are repeated for many generations, with the expectation of producing the best individual(s) that could represent the optimal or near optimal solution to the problem under study.

3 Results

3.1 Calibration of the sub-models

A/C_i response of *P. euphratica* leaves, examined at an irradiation of 1500 μmol m^{-2} s^{-1} and leaf temperature 25°C, followed typical A/C_i response patterns of C$_3$ plants (Fig. 3a). Estimates of the photosynthesis parameters were 75.09±1.36 (approximated standard error), 117.27±2.47, 8.21±0.10, and 5.81±0.08 μmolm^{-2} s^{-1} for $V_{c\,max}$, J_{max}, TPU, and R_d at 25°C, respectively. The FvCB sub-model described the photosynthetic response very well over a range of measured C_i at 25°C. The transition points from A_c to A_j and from A_j to A_p occurred at 23.2 and 88.3 Pa, respectively (Fig. 3a). The model response to irradiation was also examined at C_i of 38 Pa at 25°C. From Fig. 3b, we can see that the model simulated fairly well and transition from RuBP-limited to Rubisoco-

limited or TPU-limited photosynthesis did not occur during doing light response curves under these circumstances.

Figure 4a shows the relationship between stomatal conductance (g_{sw}) and the stomatal index (Ah/C_s) of the BWB sub-model of *P. euphratica*. The optimized values for parameters m and $g_{sw\,min}$ are 11.32 and −0.0091, respectively. The BWB sub-model was capable of accounting for 92% of the observed variation in measured stomatal conductance of calibration data (Fig. 4b).

3.2 Model validation

3.2.1 Prediction of A by the FvCB model

Predicted A by the FvCB model is represented graphically against calibration data (Fig. 5). At 10°C, A was insensitive to high CO_2 levels. The FvCB sub-model simulated this observed pattern well; that is, an increase of photosynthesis rated up to the CO_2 concentration level about 20.7 Pa, followed by a flat line as CO_2 increased further (Fig. 5a). The model predicted a flat response at high CO_2 levels as a result of a limitation due to A_p. At 10°C, the model predicted a nearly direct transition from the Rubisco-limited (A_c) to the TPU-limited (A_p) region, with a brief period of RuBP limitation (A_j, 10.4–20.7 Pa of C_i) between the two regions. At 20°C, the model behaved such that the transition from A_c to A_j occurred around 17.6 Pa and the transition between A_j and A_p took place around 54.2 Pa (Fig. 5a). At 30°C, the limitation due to A_j was recognized over a board range of CO_2 pressure from 23.8 Pa to 87.6 Pa (Fig. 5b). At 40°C, the model predicted a directly transition from A_c to A_p occurred at 29.9 Pa and the limitation due to A_j was not realized (Fig.5b). The model successfully reproduced the observed pattern of A/C_i responses at all four leaf temperatures.

The photosynthesis response to leaf temperature was simulated fairly well over the entire range of temperatures at various ambient CO_2 concentrations (Fig. 5c). At $C_i=100$ Pa, the optimal leaf temperature that yields the maximal net photosynthetic rate of 24.59 μmol m^{-2} s^{-1} was around 32°C. At $C_i=38$ Pa, the optimal leaf tempera-

ture increased to 34°C with a maximal photosynthetic rate of 21.32 μmol m^{-2} s^{-1}. At C_i=20 Pa, the optimal leaf temperature decreased to 23°C with a maximal photosynthetic rate of 10.0 μmol m^{-2} s^{-1}. The model response to irradiation was also simulated fairly well. At 20°C, the model predicted that A was solely limited by A_j throughout

5 all irradiation levels (Fig. 5d). At 30°C, the transition from A_j to A_c occurred around Q=820 μmol m^{-2} s^{-1}. At 40°C, the transition from A_j to A_c occurred at lower irradiation (Q=820 μmol m^{-2} s^{-1}).

3.2.2 Coupling model validation

Having parameterized the combined model as described above, we simulated the diur-
10 nal courses of photosynthesis and evapotranspiration on a leaf scale, using as driving variables the measured values of the leaf temperature and irradiation, as well as measured C_s and h. The resulting simulations were compared with the measure rates of net photosynthesis (Fig. 6a) and transpiration (Fig. 6b). The combined model successfully reproduced the observed response in A. Of note, the observed net assimilation rate
15 of the *P. euphratica* leaves peaked at 10:00 LT and declined gradually until 15:00 LT with a slightly increase after that. The regression line slope between the observed and modeled values was 1.01 with an intercept of −0.0807 (Fig. 7a). However, the combined model generally tended to overestimate the transpiration (Fig. 6b) and the regression line slope deviated significantly from unity (Fig. 7b). Comparing the daily
20 integrated totals of carbon fixed and water lost, the model overestimated daily CO_2 fixation by 0.44% and underestimated water loss by 9.31%, respectively. Overall, the combined model generally captured the diurnal patterns of CO_2 and H_2O exchange resulting from variation in temperatures and irradiation.

4 Discussion

4.1 Model parameterization

The major advantage of the proposed method is its global nature, and its ability to outperform simultaneous estimates. Our experiments showed that the appropriately identifying bounds on parameters for minimization in proximity to the global minimum were indispensable. Wide bounds may have some utility in keeping the minimization from drifting into nonsensical ranges. In very rare circumstances, data include samples of three segments, but wide bounds result in an A/C_i set for which two (one) of the three functions happen(s) to provide a better fit than three functions combined, despite the underlying presence of three phases (Su et al., 2009). In this circumstance, we say the GA method obtained biologically implausible estimates for the parameters of the FvCB model.

It is possible to prohibit the estimation procedure from reaching biologically implausible values by constraining the range of a parameter. Knowing the initial value of A/C_i curve, one can use the following equation to get an approximate estimation for $V_{c\,max}$ (when C_i equals to the CO_2 compensation point Γ^*):

$$V_{c\,max,0} = \frac{dA}{dC_i}(\Gamma^* + K_c(1 + O/K_O)) \, , \tag{12}$$

where $V_{c\,max,0}$ is the primary estimation of $V_{c\,max}$, $\frac{dA}{dC_i}$ is the initial slope of the A/C_i curve, which can be calculated from the difference quotient of the first two points of the A/C_i curves.

When $C_i \to +\infty$, A_j in Eq. (3) becomes

$$\lim_{C_i \to +\infty} A_j = \lim_{C_i \to +\infty} \frac{J}{4} \frac{C_i - \Gamma^*}{C_i + 2\Gamma^*} = \frac{J}{4} \, , \tag{13}$$

where $\lim_{C_i \to +\infty} A_j$ is the limit of the RuBP-limited photosynthesis rate function when

Title Page

Abstract | Introduction

Conclusions | References

Tables | Figures

|◄ | ►|

◄ | ►

Back | Close

Full Screen / Esc

Printer-friendly Version

Interactive Discussion

$C_i \to +\infty$, which can be approximately evaluated from the last two end points on the A/C_i curves. Thus J_{max} can be approximately estimated by:

$$J_{max,0} = 4 \lim_{C_i \to +\infty} A_j \,, \tag{14}$$

where $J_{max,0}$ is the primary estimation of J_{max}.

5   If TPU-limited photosynthesis occurs as no increase in A with increasing CO_2 concentration, approximate TPU value can be easily obtained:

$$TPU_0 = \frac{A_p}{3} \,. \tag{15}$$

Generally, R_d is constrained to be greater than 0 and less than $10\,\mu\mathrm{mol\,m^{-2}\,s^{-1}}$ (Sharkey et al., 2007). Thus, for any given A/C_i curves, the bounds for parameters

10   $V_{c\,max}$, R_d, J_{max} and TPU are $[V_{c\,max,0}-30, V_{c\,max,0}+40]$, $[0, 10]$, $[J_{max,0}-40, J_{max,0}+70]$ and $[TPU_0-3, TPU_0+3]$. Our experiences showed that at these search spaces the optimum parameters were all successfully found at one time.

The BWB model is empirical and has received wide attention, analysis, acceptance and applications (Muchow, 1985; Lhomme et al., 1998). The applications of the model

15   to CO_2 and H_2O exchange studies result in coupled equations which required recursive or iterative computation. Thus, it may not be favourable for large-scale ecosystem simulations. Also, the empirical nature of the BWB model makes it difficult to extrapolate the model into future environmental regimes. For example, the effect of the soil water stress on stomatal conductance was not explicitly included in the model.

20   ## 4.2 Maximum carboxylation rate, $V_{c\,max}$ and maximum rate of electron transport, J_{max}

Values for $V_{c\,max}$ of 75.09 ± 1.36 and J_{max} of $117.27\pm2.47\,\mu\mathrm{mol\,m^{-2}\,s^{-1}}$ were obtained for *P. euphratica* leaves at 25°C. It should be noticed that the assessed values of $V_{c\,max}$ and J_{max} at a reference temperature dependent on the choice of the Rubisco

kinetic parameters and temperature dependence functions in each model. Therefore, care should be needed for the comparison of the $V_{c\,max}$ and J_{max} with other studies. Wullschleger's list of $V_{c\,max}$ and J_{max} for 109 species estimated from the A/C_i curves included five species from the genus *Populus* (Wullschleger, 1993). Our values of

5    $V_{c\,max}$ and J_{max} for *P. euphratica* is very close to Wullschleger's two values for *Populus* species (Table 2). The optimal $V_{c\,max}$ and J_{max} for *P. euphratica* in this study are also close to Wullschleger's values for hardwood in temperate forests of *Betura pendula* and *Quercus rubra*.

     Various functions have been used to describe the temperature dependence of $V_{c\,max}$

10   and J_{max}. For example, Harley et al. (1992) and Leuning (1995) employed a compound function with an optimum for both $V_{c\,max}$ and J_{max}, whereas de Pury and Farquhar (1997) used an exponential growth function for $V_{c\,max}$. Leuning (2002) reported that functions describing temperature responses of the photosynthetic parameters $V_{c\,max}$ and J_{max} at 25°C showed little variation between different species at leaf temperatures

15   <30°C, while above this temperature variation was large and species-dependent. Under the natural condition, better predictions of Rubisoc-limited photosynthesis are necessary because of the synchronous variations of temperatures and irradiation, thus, photosynthesis is commonly Rubisco-limited. In our experiments, we found a slight decline of $V_{c\,max}$ when the temperature was greater than 40°C. However, we opted to use

20   the exponential function because it resulted in better overall performance for the typical diurnal gas exchange on a leaf scale. The leaf nitrogen content can also be linked to key photosynthetic model parameters such as $V_{c\,max}$ and J_{max} (Gonzalez-Real and Baille, 2000). Therefore, further studies are still needed to reveal these relationships.

4.3 Parameters of BWB sub-model

25   Table 3 compared the optimized values of parameters m and $g_{sw\,min}$ for BWB sub-model with other studies. Parameter m in the BWB sub-model for *P. euphratica* is 11.31. This value is in the range of values for C_3 tree species listed in Table 3. Evidence from gas exchange measurements suggests that the value of m occupies a relatively

narrow range for all C_3 species. Based on this, some noteworthy studies simulating canopy fluxes used a constant m of around 9 (see also Table 3). Nevertheless, parameter m has a significant physiological meaning related to the intrinsic water use efficiency, indicating a plant-specific manner of regulating the fluxes, and the importance of slight fluctuation in parameter m should not be undervalued (Kosugi et al., 2003). Studies have reported that the soil and plant water status might effect m through regulating leaf water potentials. Results showed that m became small during soil drought conditions (Sala and Tenhunen, 1996) and in old tress (Falge et al., 1996). Thus, Gao et al. (2002) derived a new model for the plant stomatal conductance and transpiration as a function of the soil water stress, vapour pressure deficit and photosynthetic active radiation. In the applications of the model, some additional experiments are needed in future studies.

5   Conclusions

This paper applied a combined model to simulate CO_2 and H_2O fluxes at the leaf scale for *P. euphratica*. The parameters of the FvCB sub-model were estimated by using the GA method. It is demonstrated that this method can effectively find higher quality parameter values of the FvCB sub-model based on the entire A/C_i curves data sets while obviating the need for arbitrary determination of transition points and sub-setting of the data before analysis. Moreover, the present coupled gas exchange model for *P. euphratica* leaf is capable of predicting photosynthesis, the stomatal conductance and transpiration as a function of radiation, leaf temperatures, ambient CO_2, and relative humidity, but predictions of the stomatal conductance and transpiration are less satisfactory. In the present study, the FvCB sub-model was parameterized by using A/C_i data sets under a controlled environment. Recent advances in potable equipment enabled us to make long-term field gas exchange measurements and we have been accumulating data. What about the GA method using the long-term data obtained from in situ observations of the diurnal changes in the CO_2 and H_2O fluxes in

the parameterization of the FvCB model? A comprehensive study is still required.

References

Baldocchi, D. and Meyers, T.: On using eco-physiological, micrometeorological and biogeo-chemical theory to evaluate carbon dioxide, water vapor and trace gas fluxes over vegetation: a perspective, Agr. Forest Meteorol., 90, 1–25, 1998.

Ball, J. T., Woodrow, I. E., and Berry, J. A.: A model predicting stomatal conductance and its contribution to the control of photosynthesis under different environmental conditions, in: Progress in Photosynthesis Research, edited by: Biggins, I., Martinus-Nijhoff Publishers, Dordrecht, The Netherlands, 221–224, 1987.

Barth, N. H.: Oceanographic experiment design II: Genetic algorithms, J. Amtos. Ocean. Tech., 9, 434–443, 1992.

Bernacchi, C. J., Singsaas, E. L., Pimentel, C., Portis Jr., A. R., and Long, S. P.: Improved temperature response functions for models of Rubisco-limited photosynthesis, Plant Cell Environ., 24, 253–259, 1992.

Cannell, M. G. R. and Thornley, J. H. M.: Temperature and CO_2 responses of leaf and canpony photosynthesis: a clarification using the non-rectangular hyperbola model of photosynthesis, Ann. Bot.-London, 82, 883–892, 1998.

Chen, Y. P., Chen, Y. N., Li, W. H., and Xu, C. C.: Characterization of photosynthesis of *Populus euphratica* grown in the arid region, Photosynthetica, 44(4), 622–626, 2006.

Chen, Y. N., Wang, Q., Ruan, X., Li, W. H., and Chen, Y. P.: Physiological response of *Populus euphratica* to artificial waterrecharge of the lower reaches of Tarim River, Acta Bot. Sin., 46, 1393–1401, 2004.

Cieniawski, S. E., Eheart, J. W., and Ranjithan, S.: Using genetic algorithms to solve a multi-objective groundwater monitoring problem, Water Resour. Res., 31, 399–409, 1995.

Collatz, G. J., Ball, J. T., Grivet, C., and Berry, J. A.: Physiological and environmental regulation

of stomatal conductance, photosynthesis and transpiration: a model that includes laminar boundary layer, Agr. Forest Meteorol., 54, 107–136, 1991.

De-Pury, D. G. and Farquhar, G. D.: Simple scaling of photosynthesis from leaves to canopies without the errors of big-leaf models, Plant Cell Environ., 20, 537–337, 1997.

5 Dubois, J. J. B., Fiscus, E. L., Booker, F. L., Flowers, M. D., and Reid, C. C.: Optimizing the statistical estimation of the parameters of the Farquhar-von Caemmerer-Berry model of photosynthesis, New Phytol., 176, 402–414, 2007.

Falge, E., Graber, W., Siegwolf, R., and Tenhunen, J. D.: A modelof the gas exchange response of Picea abies to habitat condi-tions, Trees, 10, 277–287, 1996.

10 Farquhar, G. D., von-Caemmerer, S., and Berry, J. A.: A biochemical model of photoshynthetic CO_2 assimilation in leaves of C_3 species, Planta, 149, 78–90, 1980.

Gao, Q., Zhao, P., Zeng, X., Cai, X., and Shen, W.: A model of stomatal conductance to quantify the relationship between leaf transpiration, microlimate and soil water stress, Plant Cell Environ., 25, 1373–1381, 2003.

15 Goldberg, D. E.: Genetic Algorithms in Search, Optimization and Machine Learning, Addison-Wesley Longman Publishing Co., Inc., Boston, MA, USA, 1989.

Gu, R. S., Liu, Q. L., Pei, D., and Jiang, X. N. Understanding saline and osmotic tolerance of *Populus euphratica* suspended cells, Plant Cell Tiss. Org., 78, 261–265, 2004.

Harley, P. C., Tenhunen, J. D., and Lange, O. L.: Use of an analytical model to study limitation on 20 net photosynthesis in *Arbutus unedo* under field conditions, Oecologia, 70, 393–401, 1986.

Harley, P. C., Thomas, R. B., Reynolds, J. F., and Strain, B. R.: Modelling photosynthesis of cotton grown in elevated CO_2, Plant Cell Environ., 15, 271–282, 1992.

Holland, J. H.: Adaptation in natural and artificial systems, The University of Michigan Press, Ann Arbor, MI, 1975.

25 Hu, B., Tang, G., Ma, J. W., and Yang, H. Z.: Parametric inversion of viscoelastic media from VSP data using a genetic algorithms, Appl. Geophys., 4(3), 194–200, 2007.

Kattge, J. and Knorr, W.: Temperature acclimation in a biochemical model of photosynthesis: a reanalysis of data from 36 species, Plant Cell Environ., 30, 1176–1190, 2007.

Kim, S. K. and Lieth, J. H.: A coupled model of photosynthesis, stomatal conductance and 30 transpiration for a rose leaf (*Rosa hybrida* L.), Ann. Bot.-London, 91, 771–781, 2003.

Kosugi, Y., Shibata, S., and Kobashi, S.: Parameterization of the CO_2 and H_2O gas exchange of several temperate deciduousbroad-leaved trees at the leaf scale considering season-alchanges, Plant Cell Environ., 26, 285–301, 2003.

Parameterization of the coupling CO_2 and H_2O exchange model

G. Zhu et al.

Full Screen / Esc

Printer-friendly Version

Interactive Discussion

Lee, Y. H., Park, S. K., and Chang, D.-E.: Parameter estimation using the genetic algorithm and its impact on quantitative precipitation forecast, Ann. Geophys., 24, 3185–3189, 2006, http://www.ann-geophys.net/24/3185/2006/.

Leuning, R.: A critical appraisal of combined stomatal-photosynthesis model for C$_3$ plants, Plant Cell Environ., 18, 339–355, 1995.

Lhomme, J. P., Elguero, E., Chehbouni, A., and Boulet, G.: Stomatal control of transpiration: examination of Monteith's formulation of canopy resistance, Water Resour. Res., 34, 2301–2308, 1998.

Long, S. P., Postl, W. F., and Bolharnordenkampf, H. R.: Quantum yields for uptake of carbon dioxide in C$_3$ vascular plants of contrasting habitats and taxonomic groupings, Planta, 189, 226–234, 1993.

Ma, T. J., Liu, Q. L., Li, Z., and Zhang, X. J.: Tonoplast H+-ATPase in response to salt stress in *Populus euphratica* cell suspensions, Plant Sci., 163, 499–505, 2002.

Makino, A., Nakano, H., and Mae, T.: Effects of growth tem-perature on the responses of ribulose-1,5-bisphosphate carbox-ylase, electron transport components, and sucrose syn-thesisenzymes to leaf nitrogen in rice, and their relationships to pho-tosynthesis, Plant Physiol., 105, 1231–1238, 1994.

Medlyn, B. E., Dreyer, E., Ellsworth, D., Forstreuter, M., Harley, P. C., Kirschbaum, M. U. F., Leroux, X., Montpied, P., Strassemeyer, J., Walcrofi, A., Wang, K., and Loustau, D.: Temper-ature response of parameters of a biochemically based model of photosynthesis: II. A review of experimental data, Plant Cell Environ., 25, 1167–1179, 2002.

Muchow, R. C.: Stomatal behavior in grain legumes grownunder different soil water regimes in a semi-arid tropical envi-ronment, Field Crop. Res., 11, 291–307, 1985.

Ooka, R. and Komamura, K.: Optimal design method for building energy systems using genetic algorithms, Build. Environ., 44, 1538–1544, 2009.

Sala, A. and Tenhunen, J. D.: Simulations of canopy net photo-synthesis and transpiration in Quercus ilex L. under the influence of seasonal drought, Agr. Forest Meteorol., 78, 203–222, 1996.

Sellers, P. J., Randall, D. A., Collatz, G. J., Berry, J. A., Field, C. B., Dazlich, D. A., Zhang, C., Collelo, G. D., and Bounoua, L.: A revised land surface parameterization (SiB2) for atmo-spheric GCMs. Part I: Modeling formulation, J. Climate, 9, 676–705, 1996.

Sharma, A., Dwivedi, B. N., Singh, B., and Kumar, K.: Introduction of *Populus euphratica* in Indian semi-arid trans angetic plains, Ann. Forest., 7, 1–8, 1999.

Title Page

Abstract | Introduction

Conclusions | References

Tables | Figures

◄◄ | ►►

◄ | ►

Back | Close

Full Screen / Esc

Printer-friendly Version

Interactive Discussion

Su, Y., Zhu, G., Miao, Z., Feng, Q., and Chang, Z.: Estimation of parameters of a bio-chemically based model of photosynthesis using a genetic algorithm, Plant Cell Environ., doi:10.1111/j.1365-3040.2009.02036.x, accepted, 2009.

Su, Y. H., Feng, Q., Zhu, G. F., Si, J. H., and Zhang, Y. W.: Identification and evolution of groundwater chemistry in the Ejin Sub-Basin of the Heihe River, Northwest China, Pedosphere, 17(3), 331–342, 2007.

Tcherkez, G. G. B., Farquhar, G. D., and Andrews, T. J.: Despites low catalysis and confused substrate specificity, all ribulose bisphosphate carboxylases may be nearly perfectly optimized, P. Natl. Acad. Sci. USA, 103, 7246–7251, 2006.

Tenhunen, J. D., Sala, A., Harley, P. C., Doughherty, R. L., and Reynolds, J. F.: Factors influencing carbon fixation and watuse by mediterranean sclerophyll shrubs during summerdrought, Oecologia, 82, 381–393, 1990.

Von-Caemmerer, S.: Biochemical Models of Leaf Photosynthesis, CSIRO Publishing, Collingwood, Victoria, Australia, 1–165, 2000.

Wilson, K. B., Baldocchi, D. D., and Hanson, A. P. J.: Leaf ageaffects the seasonal pattern of photosynthetic capacity and netecosystem exchange of carbon in a deciduous forest, Plant Cell Environ., 24, 571–583, 2001.

Table 1. The scaling constant (c) and enthalpies of activation (ΔH_a), deactivation (ΔH_d) and entropy (ΔS) describing the temperature responses for ribulose 1·5-bisphosphate carboxylase/oxygenase (Rubisco) enzyme kinetic parameters that are necessary for A/C_i analysis over a range of temperature.

	25°C	c	ΔH_a	ΔH_d	ΔS
Parameters used for fitting					
K_c (Pa)	27.238	35.9774	80.99		
K_o (kPa)	16.582	12.3772	23.72		
Γ^* (Pa)	3.743	11.187	24.46		
Used for normalizing					
$V_{c\,max}$	1	26.355	65.33		
J_{max}	1	17.71	43.9		
TPU	1	21.46	53.1	201.8	0.65
R_d	1	18.7145	46.39		

Estimations of each parameter at 25°C are also provided. Values are taken from Bernacchi at al. (2001, 2002), Bernacchi, Pimentel and Long (2003) and also see Sharkey et al. (2007).

Table 2. A comparison of $V_{c\,max}$ and J_{max} of the investigated tress with the results of other studies.

Species	Temperature (°C)	Irradiance (μmol m^{-2} s^{-1})	$V_{c\,max}$ (μmol m^{-2} s^{-1}) Mean±the asymotic error	95%CL[a]	J_{max} (μmol m^{-2} s^{-1}) Mean±the asymotic error	95%CL[a]	Reference
P. euphratica	25	1500	75.09±1.36	–	117.27±2.47	–	From this study
Populus deltoides	30	2000	59±2	54–63	117±1	114–120	Regehr et al. (1975)
Populus grandidentata	25	1600	72±4	53–91	169±4	160–178	Jurik et al. (1984)
Betura pendila	25	1200	70.5	–	106±2	102–109	Matyssek et al. (1991)
Quercus rubra	30	700	51±15	−145–247	127±9	100–154	Loreto and Sharkey (1994)

[a] Upper and lower 95% confidence limit.

Table 3. A comparison of the parameters for BWB submodel with other studies.

Species	m	$g_{sw\,min}$	References
P. euphratica	11.32	−0.0091	From this study
Gossypium hirsutum (cotton)	9.58	0.0811	Harley et al. 1992
Quercus alba, and *Acer rubrum*	9.5	0.0175	Harley and Baldocchi 1995
Quercus ilex	15.0	0.005	Sala and Tenhunen 1996
Platanus orientalis	9.8	0.061	Kosugi, Shibata and Kobashi 2003
Liriodendron tulipifera	9.3	0.052	Kosugi, Shibata and Kobashi 2003
Quoted and used for the simulation			
C$_3$ plants	9	0.01	Sellers et al. (1996) (SiB2)
Conifers	6	0.01	
C$_4$ plants	4	0.04	
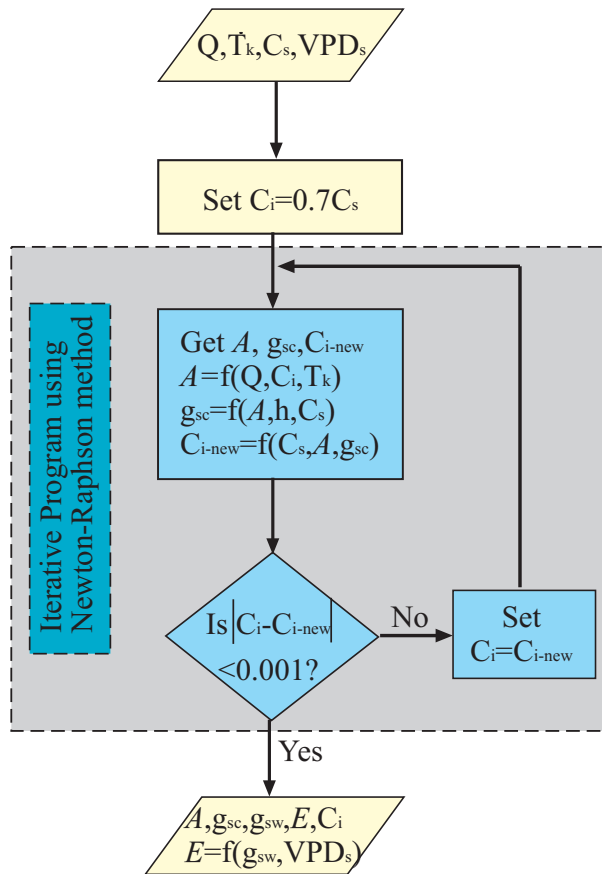
Fig. 1. Schematic diagram of the coupling models flow.
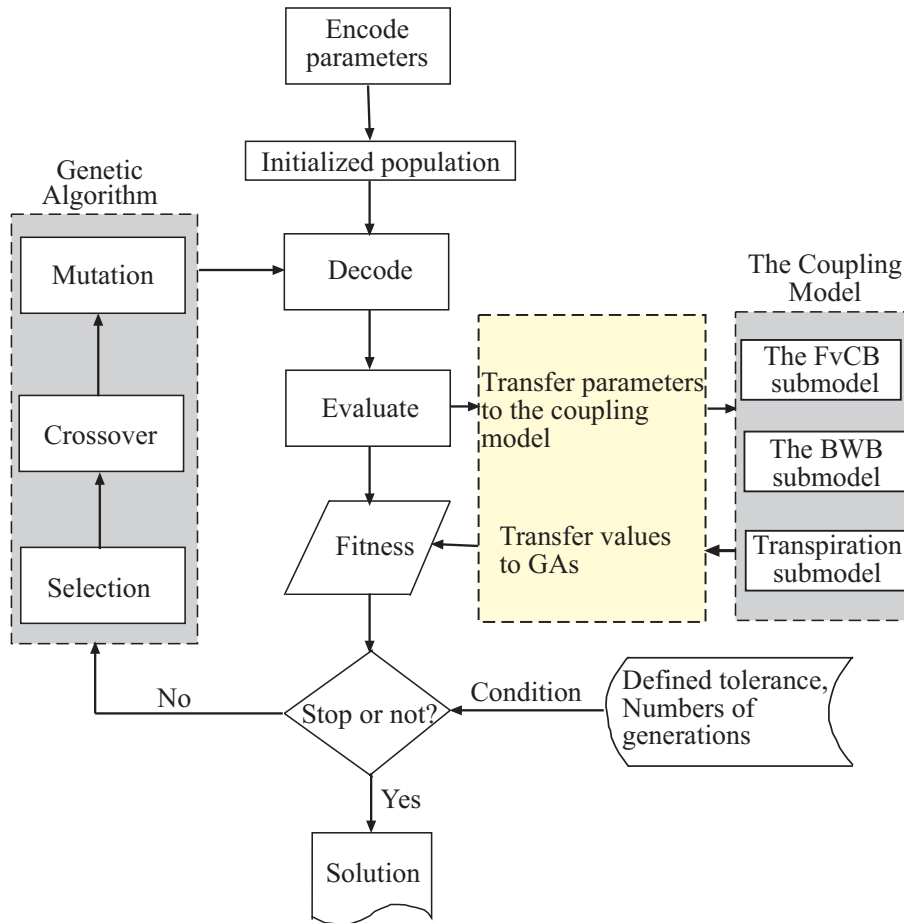
Full Screen / Esc

Fig. 2. Flow chart of the GA estimator for parameter estimation of the coupling models.
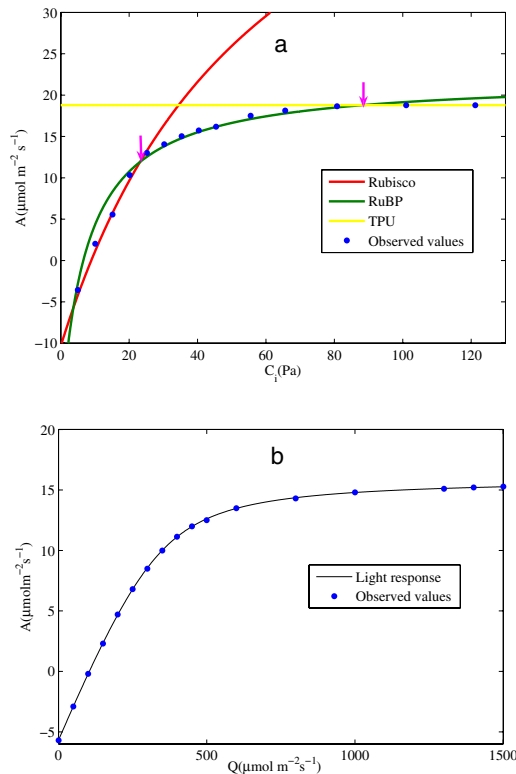
Fig. 3. Examples of genetic algorithms (GA) to A/C_i curve in parameter estimations **(a)** and corresponding light response curves **(b)**. For the A/C_i curve, the data set was properly subdivided into three subsets by GA with the photosynthesis parameters were 75.09±1.36, 117.27±2.47, 8.21±0.10, and 5.81±0.08 for $V_{c\,max}$, J_{max}, TPU, and R_d at 25°C, respectively. Points below 23.2 Pa was regarded as Rubisco-limited and above 88.3 Pa as TPU-limited; points between 23.2 and 88.3 Pa might be RuBP-regeneration-limited-the arrow indicates the transition points between different segments. Light response curve at C_i of 36.4 Pa at 25 °C.
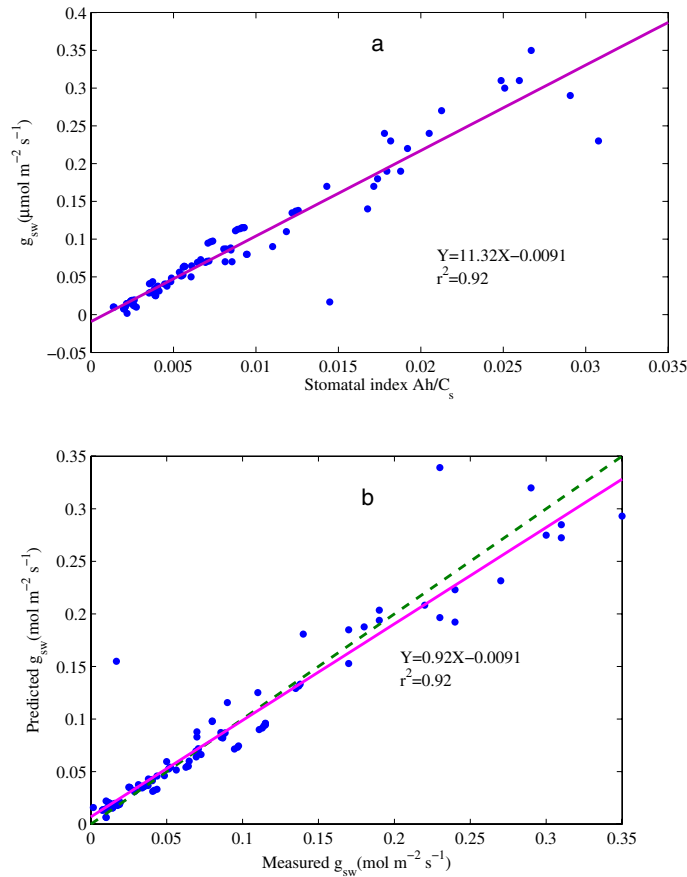
Fig. 4. Calibration of the BWB model. **(a)** Relationship between stomatal conductance and the stomatal index (Ah/C_s); **(b)** linear regression of predicted g_{sw} on measured g_{sw} as a result of BWB model calibration. Dashed line indicated 1:1 relationship.
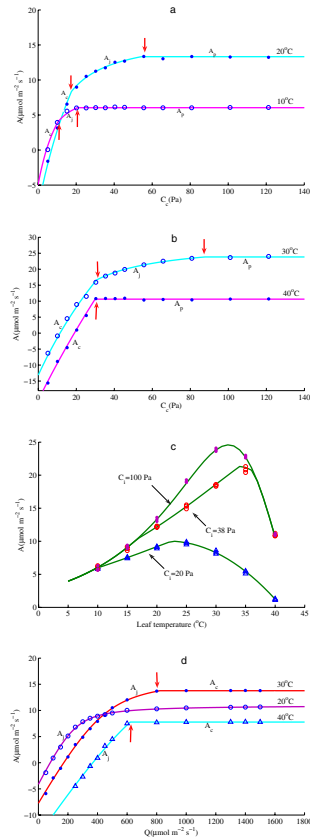
Fig. 5. Prediction of net photosynthesis (A). Lines represent the FvCB model prediction; symbols are observations of calibration data. **(a)** A/C_i responses at 10 and 20°C; **(b)** A/C_i responses at 30 and 40°C; **(c)** temperature response at three C_i levels (20, 38, and 100 Pa); **(d)** light responses at C_i=38 Pa at three leaf temperature levels (20, 30 and 40°C).
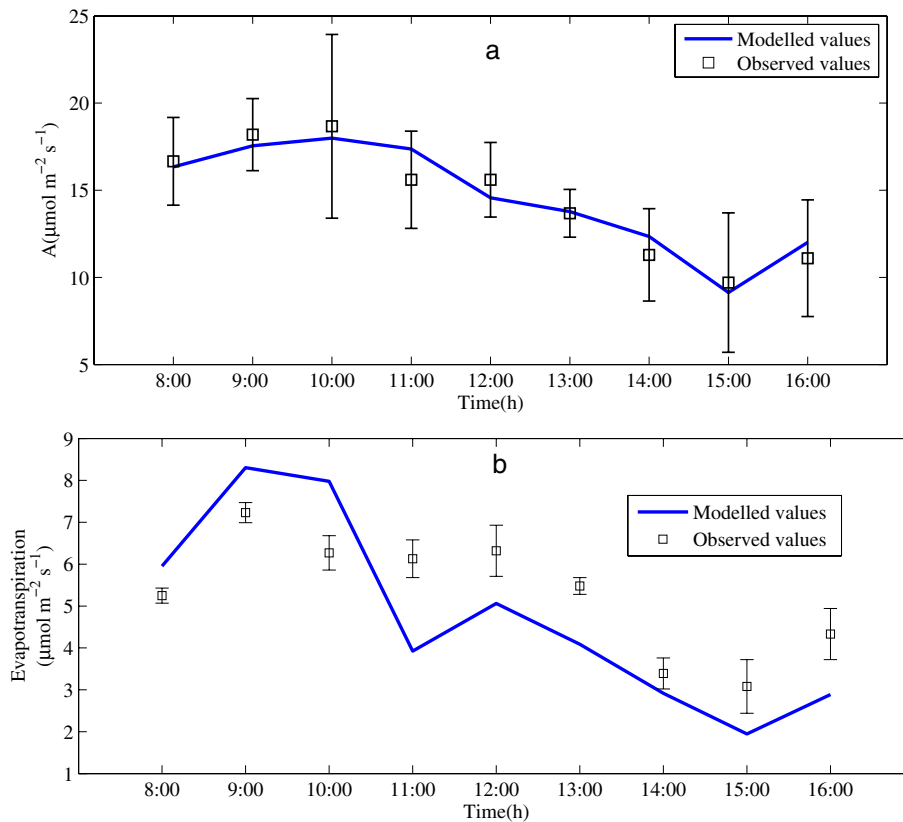
Fig. 6. Comparison of the observed and estimated **(a)** net assimilation rates and **(b)** transpiration rates using the optimized parameters obtained by GA method.
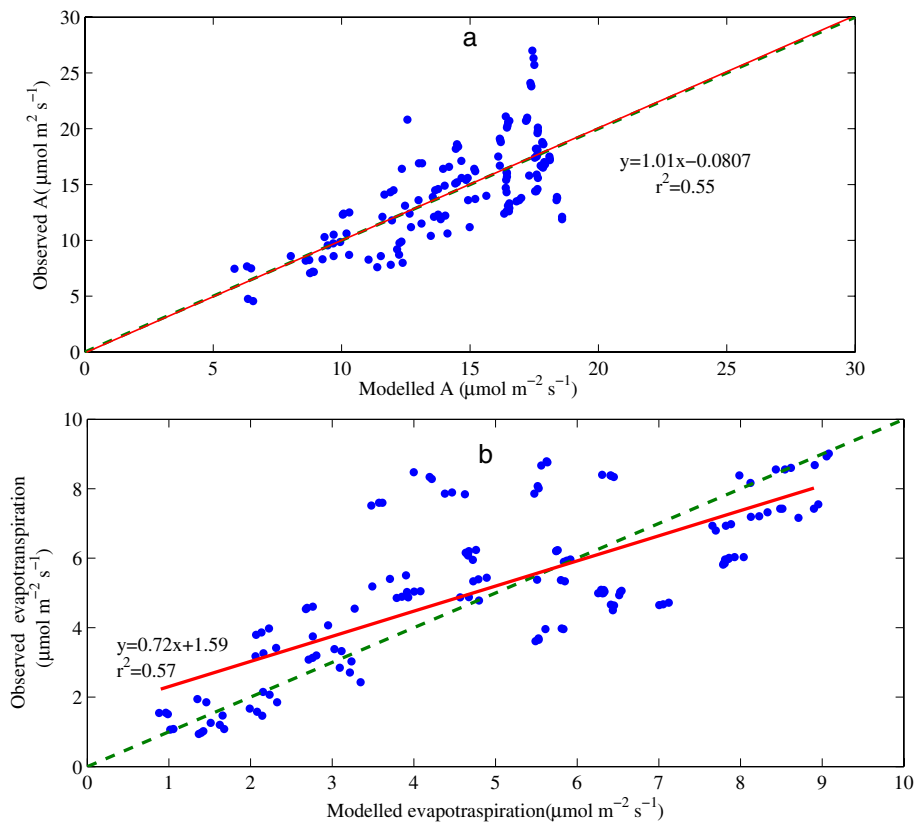
Fig. 7. Linear regression of **(a)** predicted A on measured A; **(b)** predicted transpiration on measured transpiration. Dashed line indicates one to one relationship.